Block copolymer micelle solutions: 2. An intrinsic excimer fluorescence study

Alan S. Yeung and Curtis W. Frank*
Department of Chemical Engineering, Stanford University, Stanford, CA 94305-5025, USA
(Received 10 July 1989; accepted 18 November 1989)

We have utilized photostationary and transient excimer fluorescence to extend our study of the concentration dependence of PSPEP in heptane, given in the previous paper. The concentration dependence of photostationary observables, namely the excimer-to-monomer intensity ratio I_D/I_M, the excimer bandwidth $\Delta\nu_{D,1/2}$ and the excimer band maximum position ν_D, can be explained in terms of the variation of solvent content in the core. Using a three-dimensional energy migration lattice model developed previously by Gelles and Frank in 1983 for studying miscible blends of polystyrene (PS) and poly(vinyl methyl ether), we have estimated the volume fraction of PS in the core as a function of concentration. In addition, both photostationary and transient results indicate that the free chain–micelle equilibrium is changed in favour of more free chains above 0.5% for the heptane solution and above 0.25% for the dodecane solution. The amount of free chains in the dispersed phase could also be estimated from the lattice model by a lever-rule approach. The critical micelle temperature (c.m.t.) can be measured by monitoring the changes of the excimer bandwidth at elevated temperatures. At temperatures below the c.m.t., two different transitions, in the form of small increases in I_D/I_M, were observed, and have been attributed to the solvation of the micelle core and the disordering of the core–corona interface.

(Keywords: block copolymer solutions; micelle; excimer fluorescence; concentration dependence; temperature dependence)

INTRODUCTION

In the previous paper[1], turbidity, viscosity and photon correlation spectroscopy (p.c.s.) were utilized to study the concentration dependence of the micelle formation by a diblock copolymer of polystyrene-*b*-poly(ethylene propylene) (PSPEP) in heptane. The critical micelle concentration (c.m.c.) as determined by p.c.s. was about 0.002% by weight. From turbidity measurements, we determined that the apparent micellar weight was relatively unchanged over the concentration range of $c =$ 0.01–0.5%. The unusually large hydrodynamic radius of 59.2 nm observed at $c = 0.003\%$, a concentration close to the c.m.c., was attributed to the swelling of the core by heptane.

At concentrations above 0.5%, the turbidity and specific refractive index increment dn/dc are abruptly reduced, suggesting a reduction in the molecular weight of particles in solution. This behaviour is paralleled by a pronounced increase in reduced viscosity in the same concentration region. Based on our analysis of the p.c.s. results, we have concluded that there is a change in the free chain–micelle equilibrium in favour of the free chains at concentrations above 0.7%. The amount of free chains relative to micelles appears to increase over the bulk concentration range from 0.7 up to 2%, above which the relative distribution cannot be determined unambiguously from p.c.s. measurements. Here we introduce the technique of excimer fluorescence to investigate further the concentration dependence of the free chain–micelle equilibrium.

Owing to its sensitivity on the molecular level, excimer fluorescence has proved to be effective in the study of changes in local segment density[2,3]. Despite the fact that fluorescence spectroscopy has been used extensively in studying aqueous micelles and surfactants[4–7], little work has been reported on the fluorescence behaviour of diblock copolymer micelles. With this in mind, the present study was also undertaken to characterize the intrinsic fluorescence behaviour of a PSPEP diblock copolymer in a so-called constrained geometry. We believe that this represents the first report on the intrinsic fluorescence behaviour of the PSPEP micelles. Our objective is to utilize excimer fluorescence as a tool for the elucidation of PS core morphology, as well as for the determination of the critical micelle temperature (c.m.t.) and the critical micelle concentration (c.m.c.).

EXPERIMENTAL

Materials and sample preparation

The PSPEP copolymer was kindly provided by Shell Development Co. and was prepared by hydrogenation of the isoprene block of a poly(styrene-*co*-isoprene) diblock copolymer. Details on its preparation and characterization have been outlined in paper 1[1] and will not be repeated here. s-Butylbenzene, the monomer model compound needed for the determination of monomer band shape, was purchased from Aldrich and was purified by distillation. All solvents used in this study were of spectrophotometric grade and were checked for fluorescence integrity before use.

Methods

Photostationary fluorescence data were collected at room temperature with a spectrofluorimeter that has been previously described[8]. All excimer excitation spectra were measured at an emission wavelength of 340 nm with an excitation bandwidth of 3 nm and emission bandwidth

* To whom correspondence should be addressed

0032-3861/90/112101-11

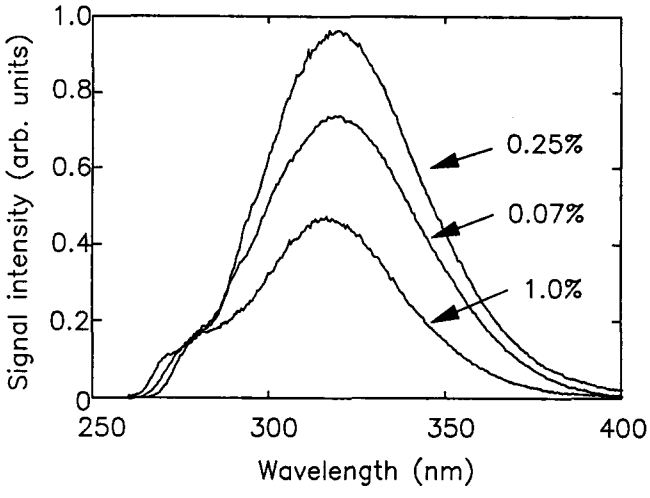

Figure 1 Typical fluorescence spectra for PSPEP in n-heptane

of 8 nm. Emission spectra were recorded with exciting light at 254 nm with bandwidths of 5 nm for both excitation and emission monochromators. An Optronic Laboratories 200 W quartz–halogen Standard of Spectral Irradiance model 220A, powered by an Optronic Laboratories model 65 constant-current power supply, was used to correct for the wavelength dependence of the quantum output of the excitation source and the spectrofluorimeter response function. The response function was confirmed by comparison of spectra of terphenol in tetrachloromethane with corrected literature spectra[9].

The integrated area ratios of excimer to monomer fluorescence, I_D/I_M, were determined according to a procedure described previously[2]. After subtraction of the Raman and scattered light peaks, the fluorescence spectra were fitted to two functional forms utilizing a non-linear regression analysis routine. The monomer band was assumed to have the same shape as the fluorescence spectrum of a 0.2 wt% s-butylbenzene solution in heptane, whereas the excimer band was assumed to be Gaussian in shape on an energy scale.

Time-resolved fluorescence measurements were made with a Photochemical Research Associates PRA 3000 nanosecond time-correlated single-photon counting spectrometer with an excitation wavelength of 250 nm and a lamp pulse half-width less than 2 ns. Details of this spectrometer have also been described previously[10]. Monomer and excimer decay curves were measured at 275 and 340 nm, respectively, to a minimum of 3×10^4 counts in the channel of maximum population. Enhanced rejection of 250 nm scattered light at 275 nm was achieved using a Toshiba UV270 high-pass filter placed in front of the stop photomultiplier tube, in addition to a Jobin–Yvon monochromator. Data analysis was carried out with iterative reconvolution techniques.

RESULTS

Fluorescence spectra for PSPEP in heptane were measured for concentrations ranging from 0.001 to 4%. Representative fluorescence spectra for the PSPEP block copolymer in heptane are illustrated in *Figure 1*. The qualitative features of the spectra are similar for all concentrations. Each fluorescence spectrum consists of a monomer band located at about 285 nm, and a broad excimer band located at about 320–325 nm. To illustrate these changes in excimer and monomer band intensities at higher concentrations, the effect of concentration on the excimer-to-monomer intensity ratio I_D/I_M is displayed in *Figure 2*. The I_D/I_M ratios for PSPEP in dodecane at concentrations above 0.04% are also shown to illustrate the solvent effect. In paper 1[1], the critical micelle concentration (c.m.c.) was taken to be approximately 0.002% for the heptane solutions, as no detectable signals of micelles were obtained at $c<0.003\%$ from p.c.s. measurements. Here we observe no abrupt change in the extent of excimer emission as I_D/I_M increases gradually from 3 at 0.001% to 4 at 0.01%. Since excimer fluorescence is sensitive to local changes in segment density, the absence of an abrupt increase in I_D/I_M at the c.m.c. may indicate that the PS segment density of freely dispersed polymer chains is similar to that in the micelle core near the c.m.c., perhaps in the form of the so-called unimolecular micelles or unimers[11]. For PSPEP in cyclohexane, a theta solvent for PS, where no micelles are formed, we found that $I_D/I_M=2.4$–2.8 for $c>0.25$ wt%. Since the dispersed polymer chains in heptane should be more collapsed than those in cyclohexane, it is possible that I_D/I_M for the dispersed chains is higher. An alternative explanation is that the true c.m.c. for this PSPEP/heptane system is considerably lower than 0.002%, and p.c.s. was not sensitive enough to detect the existence of micelles at concentrations below 0.002%. Unfortunately, this issue cannot be resolved with the sensitivity of our current photon correlation spectrometer.

Over the concentration range from 0.01 to 0.5%, a prominent rise in I_D/I_M indicates an increase in the PS segment density in the micellar core. Interestingly, a decline in I_D/I_M begins above 0.5%, in accordance with the turbidity, viscosity and p.c.s. results previously reported[1]. In paper 1[1] we define a critical concentration c_I between 0.5 and 0.7 wt% of PSPEP in heptane, above which appreciable interactions between micelles are observed. Here I_D/I_M is found to decrease from c_I to $c=2\%$, above which a slight rise in I_D/I_M is observed

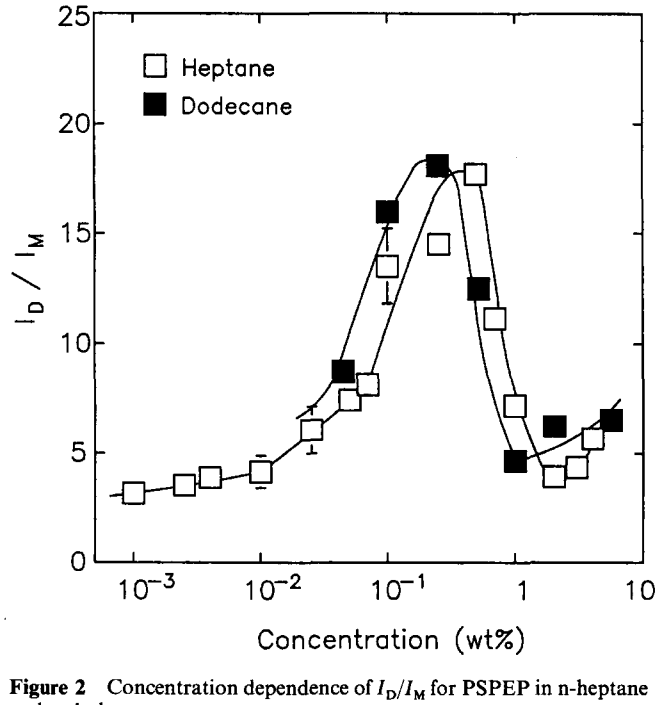

Figure 2 Concentration dependence of I_D/I_M for PSPEP in n-heptane and n-dodecane

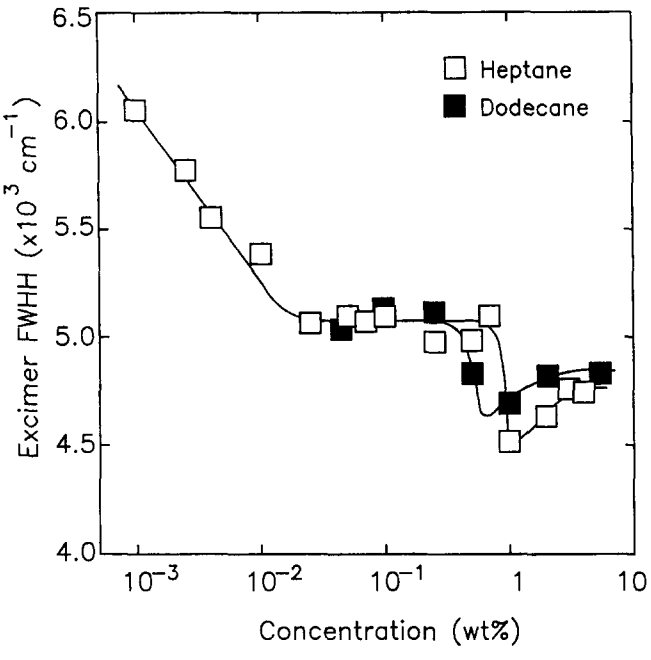

Figure 3 Concentration dependence of excimer bandwidth for PSPEP in n-heptane and n-dodecane

between 2 and 4%. As I_D/I_M is expected to be lower for the freely dispersed chains, these fluorescence observations above c_I are consistent with the suggestion, made previously in paper 1[1], that more free chains are present with increasing bulk concentration from 0.7 to 2%. As illustrated in *Figure 2*, the concentration dependence of I_D/I_M for dodecane solutions was also measured. The overall I_D/I_M behaviour for PSPEP in dodecane is similar to that for heptane, except that there appears to be a shift of the minimum of I_D/I_M from 2% for heptane solutions to about 1% for dodecane solutions.

Figure 3 shows the concentration dependence of the excimer bandwidth $\Delta\nu_{D,1/2}$ for the heptane and dodecane solutions. For the heptane solutions, we observe a significant narrowing of the excimer band from $\Delta\nu_{D,1/2} = 6000\,cm^{-1}$ at 0.001% to about $5000\,cm^{-1}$ at 0.01%. This is in contrast to the bandwidth of $\Delta\nu_{D,1/2} = 5500\,cm^{-1}$ observed for PSPEP in cyclohexane. Above 0.01%, a constant bandwidth of about $5000\,cm^{-1}$ is seen until the concentration reaches 0.7%, after which it decreases significantly. The band narrowing at 0.01 and 1% implies that rather substantial changes in the local environment as perceived by the phenyl rings take place at these points. As in the case of I_D/I_M, the dodecane solutions exhibit a bandwidth behaviour similar to the heptane solutions except for the fact that band narrowing at high concentration occurs at about 0.5% as opposed to 0.7% in heptane.

Figure 4 displays the excimer band maximum position ν_D as a function of concentration. For $c = 0.001$–0.01% we observe a blue shift of the excimer band from 3.06×10^4 to $3.10 \times 10^4\,cm^{-1}$, consistent with the changes in I_D/I_M and bandwidth observed in this region. Again, the excimer band position of the micelle solutions below $c =$ 0.01% is in agreement with the value $\Delta\nu_D = 30\,000\,cm^{-1}$ observed in cyclohexane solutions. From 0.02 to 0.5%, however, ν_D is found to be quite insensitive to polymer concentration, analogous to the constant $\Delta\nu_{D,1/2}$ over the same concentration range. These observations suggest that a constant local environment for the phenyl groups exists inside the core between 0.02 and 0.5%. The further shift of $\Delta\nu_{D,1/2}$ above c_I suggests a further change in local environment as perceived by the excimer-forming sites (e.f.s.) with concentration. Recall that the excimer bandwidth was abruptly reduced near 0.7% for heptane and 0.5% for dodecane. By contrast, the excimer band positions extracted from samples in heptane and dodecane do not show any striking dependence on the solvent size.

As a sensitive tool for probing changes in local environment, excitation spectroscopy can provide further insights into the micelle morphology. A series of excimer spectra for PSPEP in heptane are illustrated in *Figure 5*. The excitation spectra show a progressive increase of relative intensity without any appreciable change in band shape for concentrations up to 0.1%. In this region, the excitation spectra exhibit the familiar band shape typical of phenyl groups. Above 0.1%, however, this familiar band shape no longer exists, as the vibronic peaks at 240–270 nm are quenched with increasing concentration. The fact that the band shape for these excitation spectra does not change with temperature, even above the c.m.t., indicates that the absence of vibronic peaks at 240–270 nm, as well as the emergence of a small shoulder near 290 nm, may simply be artifacts of the self-absorption effect.

Figure 6 shows typical monomer decay curves at several concentrations in heptane. Evidently, the monomer decay profiles consist of a fast decay component at short times and a slow decay component at long times. The fast decay component is sometimes attributed to the quenching of monomer emission by excimer formation[12], whereas the slow decay component is thought to arise from a combination of photophysical processes such as energy migration and excimer dissociation. Nevertheless, Fredrickson has shown that, for three-dimensional energy migration, the monomer and excimer decay functions are essentially non-exponential[13]. As the monomer and excimer decay curves cannot be satisfactorily described by single- or dual-exponential decays, we will arbitrarily fit the transient data with triple-exponential decays. However, it must be emphasized that the absolute

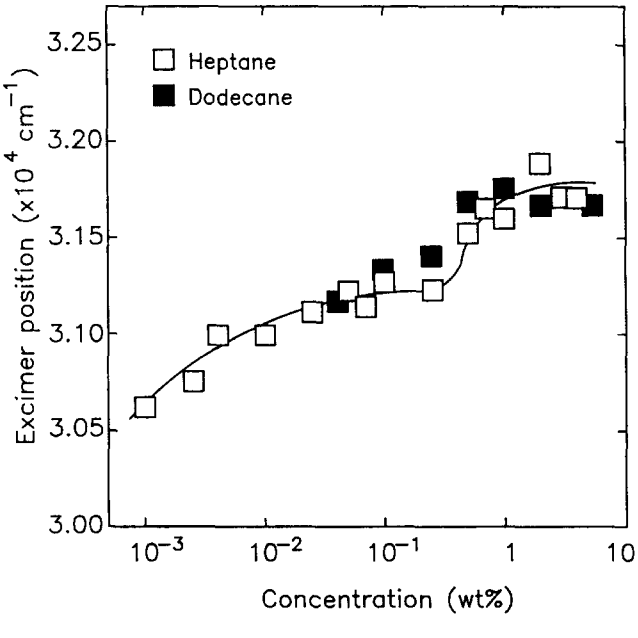

Figure 4 Concentration dependence of excimer band position for PSPEP in n-heptane and n-dodecane

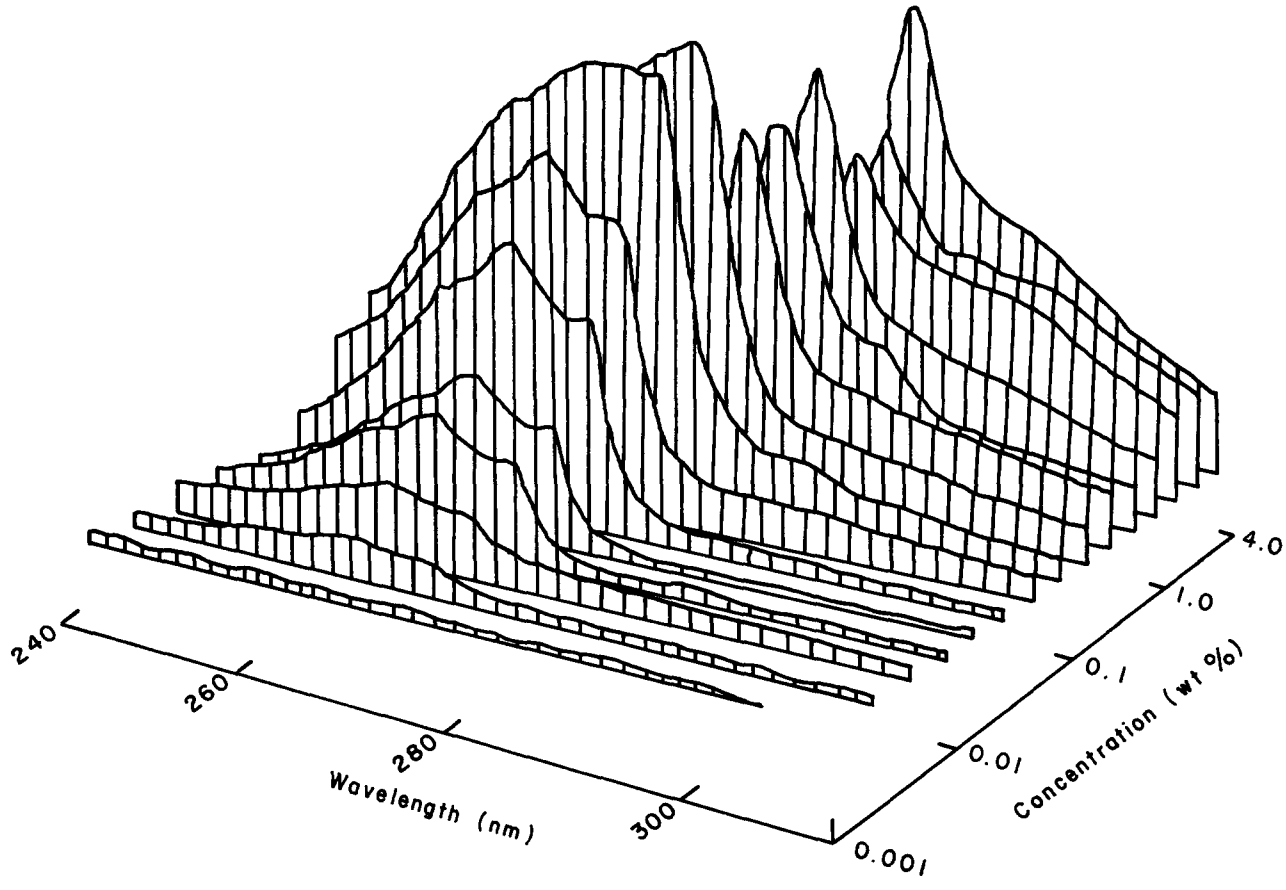

Figure 5 Excitation spectra for PSPEP in n-heptane as a function of concentration

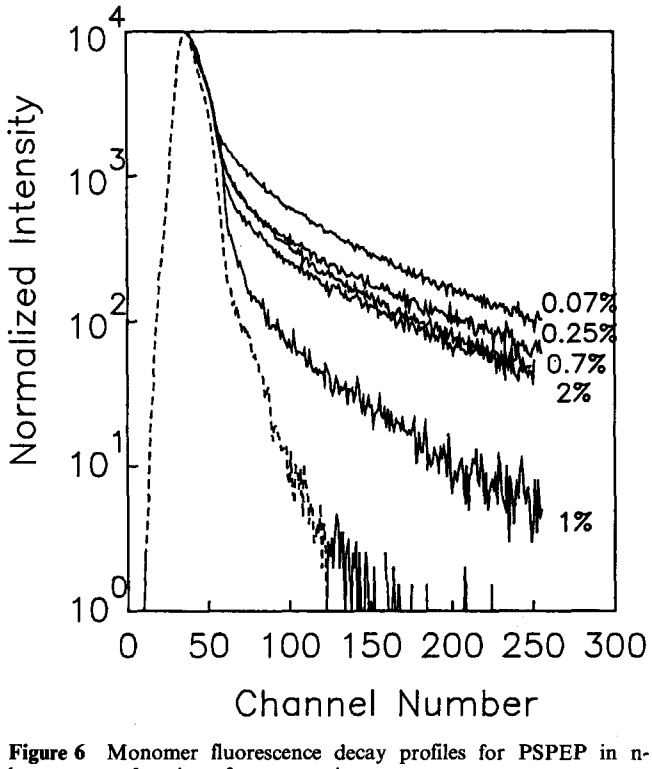

Figure 6 Monomer fluorescence decay profiles for PSPEP in n-heptane as a function of concentration

magnitudes of the fitted decay times τ_i, should not be associated with discrete excited-state decay processes.

Results from the triple-exponential fits such as the pre-exponential factors A_i, decay times τ_i, χ^2 and Durbin–Watson parameter DW for the monomer and excimer decay fits are summarized in *Tables 1* and *2*. The mean decay times $\langle\tau\rangle$, which are defined as:

$$\langle\tau\rangle = \frac{\int_0^\infty tI(t)\,dt}{\int_0^\infty I(t)\,dt} \quad (1)$$

are also included. A comparison of the monomer decay curves in *Figure 6* illustrates that the monomer fluorescence decays more rapidly with concentration, reflecting the increasing PS segment density in the core, and therefore increasing efficiency of monomer quenching. The overall trend of the transient monomer fluorescence decay can be examined from the change of $\langle\tau\rangle$ with concentration. As shown in *Figure 6*, there is a significant reduction from $\langle\tau\rangle = 7.6$ ns at 0.07% to $\langle\tau\rangle = 4.7$ ns at 0.1%. This is followed by a more moderate drop in $\langle\tau\rangle$ from 0.1 to 0.7%, in agreement with the trends of I_D/I_M, $\Delta\nu_{D,1/2}$ and ν_D discussed above. At 1% we observe a drastic decrease in $\langle\tau\rangle$, indicating that the energy migration process is very efficient, and monomer fluorescence decay is readily quenched. The apparent increase in $\langle\tau\rangle$ at 2% may be attributed to the monomer fluorescence emission of the free chains, which have become more important at this point. Although we have attempted to determine the monomer fluorescence decay above 2%, unfortunately, the monomer signal is simply too weak to be measured, partially due to the significant self-absorption effect.

The excimer decay profiles for the PSPEP solutions in heptane are shown in *Figure 7*. Although the overall excimer decay curves do not exhibit large differences in the short- and long-time decays, an inspection of the decay profiles reveals the extent of energy migration as

Table 1 Transient fluorescence decay parameters: monomer decay (excitation wavelength = 250 nm, emission wavelength = 275 nm)

Conc. (wt%)	A_1	A_2	A_3	τ_1 (ns)	τ_2 (ns)	τ_3 (ns)	$\langle\tau\rangle$ (ns)	χ^2	*DW*
0.07	0.951	0.0339	0.0151	0.38	4.71	18.6	7.63	1.221	1.746
0.10	0.976	0.0159	0.0077	0.32	4.04	16.1	4.71	1.224	1.826
0.25	0.987	0.0084	0.0043	0.20	3.05	15.5	4.01	1.184	1.901
0.50	0.993	0.0045	0.0025	0.22	3.35	14.1	3.19	1.208	1.768
0.70	0.990	0.0072	0.0017	0.13	3.22	14.1	3.13	1.212	1.948
1.0	0.995	0.0037	0.0011	0.14	2.42	16.7	2.08	1.199	2.116
2.0	0.993	0.0044	0.0022	0.14	3.02	15.0	3.09	1.082	1.893
3.0	N/A	N/A	N/A	N/A	N/A	N/A	N/A	N/A	N/A

Table 2 Transient fluorescence decay parameters: excimer decay (excitation wavelength = 250 nm, emission wavelength = 340 nm)

Conc. (wt%)	A_1	A_2	A_3	τ_1 (ns)	τ_2 (ns)	τ_3 (ns)	$\langle\tau\rangle$ (ns)	χ^2	*DW*
0.07	0.430	0.172	0.398	0.99	9.41	24.0	21.1	1.236	2.043
0.10	0.116	0.177	0.706	0.83	9.93	23.3	21.9	1.478	1.648
0.25	0.071	0.179	0.750	0.55	7.56	22.7	21.6	1.287	1.954
0.50	0.778	0.053	0.170	0.14	6.42	22.9	21.0	1.664	1.602
0.70	0.410	0.109	0.481	0.17	8.73	22.7	21.5	1.377	1.937
1.0	0.844	0.037	0.119	0.46	5.48	23.1	20.3	1.352	1.997
2.0	0.739	0.132	0.129	0.84	10.1	27.3	20.3	1.609	1.810
3.0	0.592	0.158	0.250	0.84	10.6	28.7	24.0	1.306	1.817

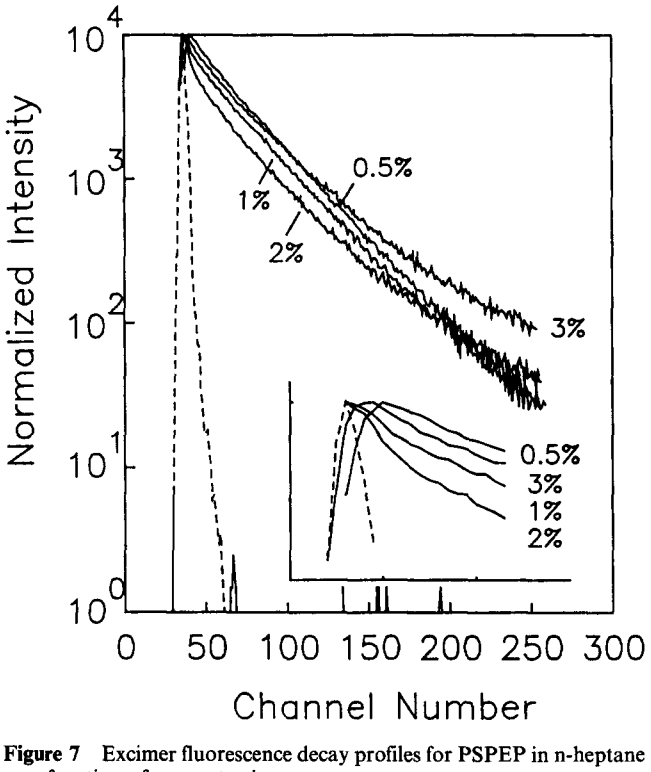

Figure 7 Excimer fluorescence decay profiles for PSPEP in n-heptane as a function of concentration

a function of concentration. For $c = 0.07$–0.5% the excimer decay profiles are qualitatively comparable, indicative of the similar pathways taken in the excimer formation process. Over this concentration range, the mean decay time is quite insensitive to bulk concentration ($\langle\tau\rangle = 21$–22 ns), indicative of the efficient energy migration that is occurring in the core. At 1 and 2%, $\langle\tau\rangle$ is somewhat reduced to 20.3 ns, whereas $\langle\tau\rangle$ increases quite noticeably to 24 ns at 3%. Perhaps more noteworthy are the considerable changes of fast decay rates at 1 and 2%. To highlight the change in rise time of excimer formation for more concentrated solutions, a comparison of excimer decay curves at short times for concentrations of 0.5, 1, 2 and 3% is also shown in *Figure 7*. Interestingly, a rise time is not observed for the excimer fluorescence decays at 1 and 2%. Such observations generally imply the existence of preformed excimer sites[2,3].

No temperature measurements for the heptane solutions are reported here, owing to the fact that the boiling temperature of heptane (372 K) is very close to the expected c.m.t. Instead, we focus our attention on the temperature dependence of excimer fluorescence for the micelle solutions in dodecane. *Figure 8* shows a plot of $\Delta\nu_{D,1/2}$ as a function of the inverse temperature for the micelle solutions in dodecane at selected concentrations. The excimer bandwidth generally broadens with temperature in all cases, more significantly for the more concentrated solutions. At the c.m.t., the thermal break-up of micelles apparently leads to a local environment wherein the e.f.s. is surrounded by more dodecane molecules, thus increasing the excimer bandwidth. This is analogous to the increase in $\Delta\nu_{D,1/2}$ when the concentration is lowered from 0.01 to 0.001% for room-temperature solutions, as shown in *Figure 3*. Owing to the dramatic band broadening at the critical micelle temperature, the excimer bandwidth lends itself to a very accurate means of determining the c.m.t. The arrows shown in *Figure 8* correspond to the intercept of the trends of bandwidth of excimer species in micellar and dispersed phases.

The temperature dependence of the excimer band position ν_D is shown in *Figure 9*. The c.m.t. for each

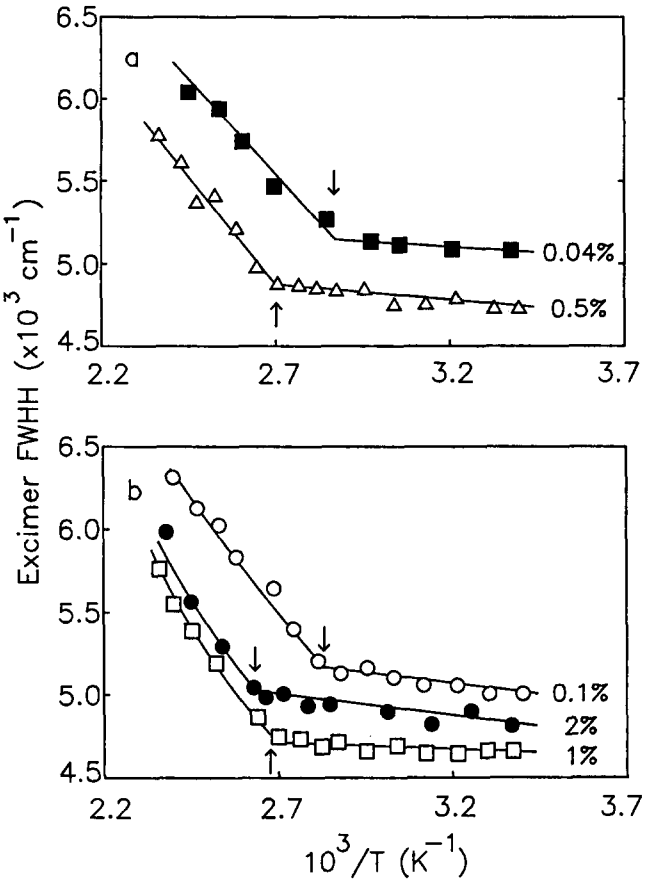

Figure 8 A comparison of excimer bandwidth as a function of temperature for 0.04, 0.1, 0.5, 1 and 2% PSPEP solutions in n-dodecane

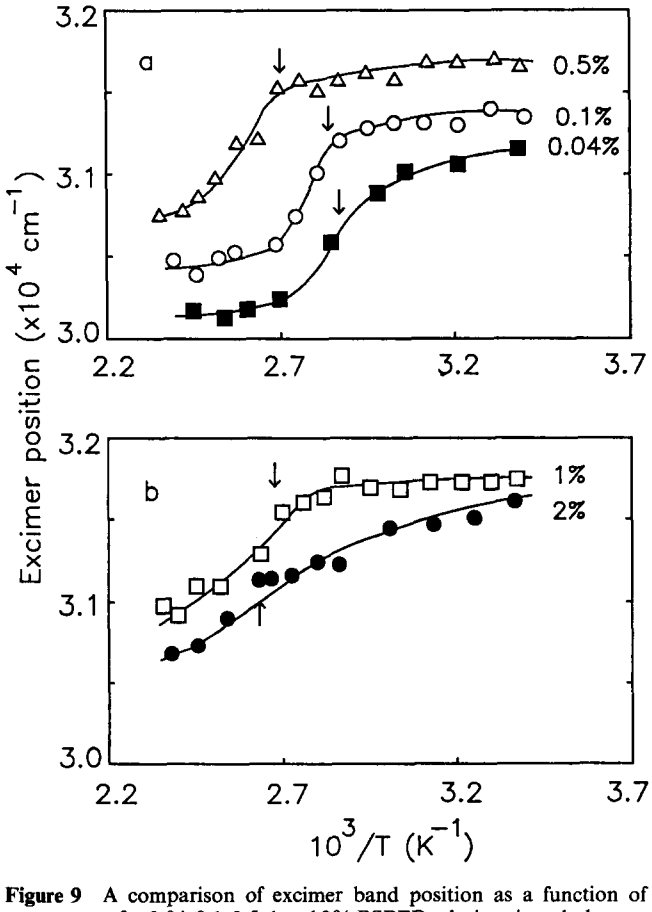

Figure 9 A comparison of excimer band position as a function of temperature for 0.04, 0.1, 0.5, 1 and 2% PSPEP solutions in n-dodecane

concentration, illustrated by various arrows, is obtained from the plot of $\Delta\nu_{D,1/2}$ vs. $1/T$ in *Figure 8*. As the temperature is raised, the excimer bands are shifted to the red, indicating that the environment within the micellar core has become more solvated and the excimer species are now of lower energy. At the c.m.t., where the micellar core is broken up, a more substantial shift of ν_D to the red results.

Figure 10 shows a plot of I_D/I_M *versus* $1/T$ for various concentrations. Also shown are values of the c.m.t. as determined from *Figure 8*. It is noteworthy that in the dodecane solutions the concentration dependence of I_D/I_M at room temperature remains qualitatively unchanged at elevated temperatures. For instance, the value of I_D/I_M for the 0.1% solution in dodecane is higher than that for the 0.5% solution at all temperatures. With the exception of the 0.04% solution, there is a small, but detectable, increase in I_D/I_M upon initial heating near 300–305 K. For each sample, practically identical fluorescence spectra were observed following such a slight rise in I_D/I_M up to about 330–350 K, where another distinct jump in I_D/I_M is observed. Increasing the temperature brings forth a gradual rise in I_D/I_M until the c.m.t. is reached. The decline in I_D/I_M at the c.m.t. may be ascribed to the thermal break-up of micelles, thus lowering the local PS segment density. Furthermore, the transitions of I_D/I_M noted at 300–305 K and 330–350 K observed in *Figure 10* are not observable in the plots of $\Delta\nu_{D,1/2}$ and ν_D against the temperature.

The determination of the c.m.t. by excimer fluorescence allows us to follow the formalism proposed by Price[14,15]

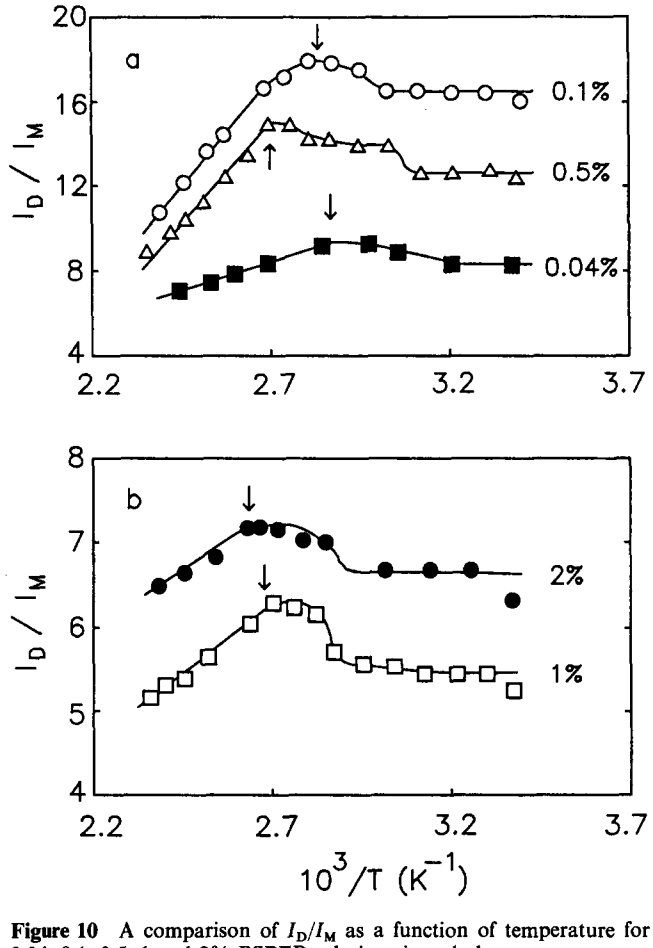

Figure 10 A comparison of I_D/I_M as a function of temperature for 0.04, 0.1, 0.5, 1 and 2% PSPEP solutions in n-dodecane

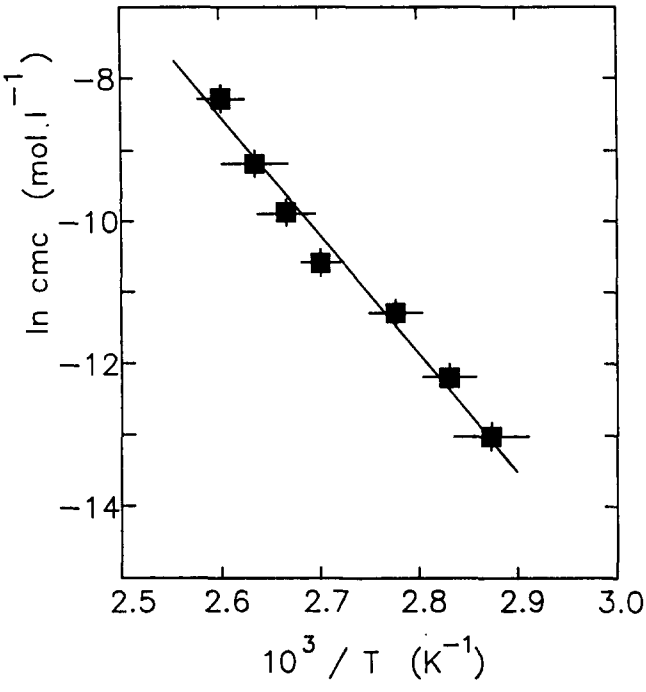

Figure 11 A plot of critical micelle concentration (c.m.c.) as a function of temperature

in estimating the standard free energy and enthalpy of micelle formation. For a closed association of micelle formation found in block copolymer micelles, the equilibrium constant between the free chains, A_1, and the micelles, A_n, is given by[14]:

$$K_n=[A_n]/[A_1]^n \tag{2}$$

such that

$$\Delta G_n^\circ = RT\ln[A_1]-\frac{RT}{n}\ln[A_n] \tag{3}$$

where ΔG_n° is the standard free-energy change per mole of copolymer on formation of an n-mer from unassociated chains.

For block copolymers, where n is large ($\sim 10^2$), the second term may be neglected, and $[A_1]$ can be taken as the c.m.c. Thus:

$$\Delta G_n^\circ = RT\ln(\text{c.m.c.}) \tag{4}$$

Since the enthalpy change of micellization, ΔH°, measured in a direct calorimetric study agrees with that obtained from the van't Hoff equation[14]:

$$\Delta H^\circ = -RT^2\frac{\mathrm{d}\ln(\text{c.m.c.})}{\mathrm{d}T} \tag{5}$$

the enthalpy change of micellization can be estimated from:

$$\ln(\text{c.m.c.})=\frac{\Delta H^\circ}{RT}+C \tag{6}$$

where C is a constant.

A plot of ln(c.m.c.), determined from *Figure 8*, against $1/T$ is given in *Figure 11*. From the slope of the plot we determined a value for the standard enthalpy of micellization $\Delta H^\circ = -136$ kJ per mole of copolymer chains. At 298 K, the standard free energy of micellization is $\Delta G^\circ = -52\,\mathrm{kJ\,mol^{-1}}$ and the standard entropy contribution is $-T\Delta S^\circ = 84.3\,\mathrm{kJ\,mol^{-1}}$. These values are in excellent agreement with those reported by Price[14]. From membrane osmometry[14], they found that, for micelles formed by a similar PSPEP block copolymer in n-decane, $\Delta H^\circ = -130\,\mathrm{kJ\,mol^{-1}}$ and $\Delta G^\circ = -42\,\mathrm{kJ\,mol^{-1}}$.

DISCUSSION

Concentration dependence of I_D/I_M

The ratio of excimer to monomer fluorescence I_D/I_M is related to the probability of eventual monomer emission M via[3]:

$$\frac{I_D}{I_M}=\frac{Q_D}{Q_M}\left(\frac{1}{M}-1\right) \tag{7}$$

where Q_D/Q_M is the ratio of intrinsic quantum yields of excimer and monomer fluorescence in the absence of interconversion between the two.

Using a lattice approach to determine the concentration dependence of the rate of energy migration and the number of e.f.s. in miscible blends of PS and poly(vinyl methyl ether) (PVME), Gelles and Frank[2] calibrated the I_D/I_M dependence on the volume fraction of PS in an amorphous phase. As migrational sampling of e.f.s. is expected to be predominant in the micellar core, we will apply such a treatment in the case of micelle formation. By doing so, we assume that the micellar core is large enough that electronic excitation transport (e.e.t.) is not appreciably modified from the infinite bulk volume treated in this model[3]. For $c=0.001$–0.5%, where essentially one phase of PS segments exists, the equation:

$$\frac{I_D}{I_M}=\frac{Q_D}{Q_M}\left(1+\frac{Nk_e}{k_M}\phi\right)\left(\frac{q_{intra}+(N-2)\zeta\phi}{1-[q_{intra}+(N-2)\zeta\phi]}\right) \tag{8}$$

provides a means to estimate the volume fraction ϕ of PS in the core. Here, N is the number of nearest neighbours, k_e is the rate constant for energy transfer to one nearest neighbour, k_M is the rate constant for monomer emission, q_{intra} is twice the probability that a dyad on the same chain is in an intramolecular e.f.s. and ζ is the probability that two adjacent rings are in an e.f.s.

For $c=0.001$–0.5%, the volume fraction ϕ of PS in the micelle core has been estimated, and the results are listed in *Table 3*. As expected, the volume fraction of PS in the core increases with concentration, from $\phi=0.4$ at 0.001% to $\phi>0.9$ at 0.5%, confirming that the micelle core is very dense and compact at sufficiently high

Table 3 Volume fraction of PS in micelle core and dispersed phase

Conc. (%)	I_D/I_M	ϕ_R[a]	X_R[a]	R_{core} (nm)
0.001	3.0	0.40	1*	13.6
0.003	3.3	0.43	1*	13.2
0.007	3.6	0.46	1*	12.9
0.010	4.0	0.50	1*	12.6
0.025	6.1	0.70	1*	11.3
0.050	7.5	0.75	1*	11.0
0.070	8.1	0.77	1*	10.9
0.10	13.5	0.88	1*	10.4
0.25	14.5	0.90	1*	10.4
0.50	15.2	0.92	1*	10.3
0.70	11.8	1*	0.95	10.0
1.0	7.1	1*	0.87	10.0
2.0	3.9	1*	0.72	10.0
3.0	4.1	1*	0.74	10.0
4.0	6.0	1*	0.84	10.0

[a] The asterisks (*) indicate assumed values

concentration. Therefore, we expect the mobility of PS segments in the core to be rather low.

For $c = 0.7$–4%, the one-phase approach can no longer be used to determine the volume fractions of PS. With no serious loss of accuracy, it can be assumed that $\phi \sim 1$ in the micelle core. In addition, we will also assume that no energy migration occurs between the core and the dispersed phase, a reasonable assumption in light of the thickness of the corona. The expression of I_D/I_M for a two-phase model is given by:

$$\frac{I_D}{I_M} = \frac{Q_D}{Q_M} \frac{X_R(1-M_R)+(1-X_R)(1-M_L)}{X_R M_R+(1-X_R)M_L} \quad (9)$$

where M_R and M_L are the probabilities of eventual monomer emission from the rich (micelle) and lean (dispersed) phases, respectively, and X_R is the fraction of phenyl rings (and therefore the copolymer) in the micelle phase.

Here, we use the values $Q_D/Q_M = 0.42$, $M_R = 0.02$ ($\phi = 1$), taken from an earlier study of miscible blends of PS and PVME[3], and $M_L = 0.14$, based on the results obtained from cyclohexane solutions, to determine the fraction of PS in the micellar core, X_R; the results are listed in *Table 3*. The ratio Q_R/Q_M is taken to be invariant since the monomer and excimer quantum efficiencies for pyrene are relatively constant in nonane and benzene[16]. The fraction of PS in the micelle phase decreases from 0.95 at 0.7% to 0.72 at 2%, after which it increases to $X_R = 0.84$ at 4%. The values of X_R obtained here are in excellent agreement with those obtained from p.c.s. measurements in paper 1[1]. Furthermore, the value of $X_R = 0.84$ at 4% is also in reasonable agreement with $X_R = 0.73$ reported for a 4% PSPEP solution in dodecane by SANS[17]. These calculations further support the proposal that the presence of free chains in the dispersed phase is driven by the concentration gradient of PEP segments. Such a driving force should diminish when the concentration is high enough for the micelles to be in contact, such as in a macrolattice, as previously described in paper 1[1].

To determine the consistency of these calculations, we have computed the radius of micelle core using:

$$R_{core} = \left(\frac{0.37 M_m}{\frac{4}{3}\pi X_R N_A}\right)^{1/3} \quad (10)$$

where R_{core} is the radius of the micelle core, M_m is the micellar weight and N_A is Avogadro's number. The values of $R_{core} = 10$–14 nm are in good agreement with the SANS results for PSPEP micelles in dodecane[17,18].

Although the agreement of X_R with the p.c.s. results is quite satisfying, it seems appropriate to comment on the validity of applying such a lattice e.e.t. model, originally developed for the solid-state amorphous blends, in the studies of the micelle microstructure. Here we have applied the model to the calculation of the volume fraction in the core below 0.01%, where I_D/I_M is below 5 and therefore ϕ is lower than 0.6[2], despite the fact that the lattice e.e.t. model is expected to work for $0.6 < \phi < 1.0$ only[3]. Furthermore, for $c < 0.01$%, where the micellar core may be swollen with solvent molecules, the phenyl rings may possess sufficient chain mobility that the rotational sampling of e.f.s. may no longer be neglected. Therefore, the estimates of ϕ at $c < 0.01$% should be viewed with some caution. Judging from the reasonable results obtained for ϕ between 0.01 and 0.5%, and for X_R between 0.7 and 4%, the assumption of infinite bulk volume for e.e.t. appears to be valid for the current values of micelle core radius. According to Gelles[3], the expected number of migrational steps experienced prior to excimer formation is between 2 and 3 for $0.6 < \phi < 1.0$. Since the Förster radius for e.e.t. in PS is approximately 0.65 nm[3,19], the assumption of infinite volume within the core should be valid for $R_{core} = 10$–14 nm. Finally, in applying the three-dimensional lattice approach, we have neglected the possibility that the PS chain segments may be somewhat stretched radially. Unfortunately, the validity of this assumption cannot be tested at this point.

Concentration dependence of $\Delta\nu_{D,1/2}$ and ν_D

Undoubtedly the most important issue here concerns the influence of the local environment on $\Delta\nu_{D,1/2}$ and ν_D. Therefore, we offer a qualitative explanation for the influence of solvent molecules on the excimer band in terms of the excimer potential energy diagram originally proposed by Birks[20].

The potential energy of a pair of phenyl rings $^1M^*$ and ^1M can be qualitatively described as a function of their separation distance r. At infinite separation, there are no interchromophoric interactions, and $^1M^*$ has an energy of M_0, corresponding to the 0–0 monomer fluorescence transition. At closer distances there is a repulsive potential $R(r)$ between the two phenyl rings due to van der Waals forces. However, the repulsive potential has not been treated theoretically, but is generally taken as the van der Waals repulsion as the two phenyl rings approach each other closer than the sum of their van der Waals radii[16]. Thus:

$$R(r) = \alpha/r^{12} \quad (11)$$

where α is a constant. In dealing with the repulsive potential under different environments, such as in solutions, however, the effect of chromophore–solvent interactions must be considered.

According to Birks[16], the stabilization of the benzene excimer is primarily due to charge resonance, and the excimer interaction potential can be approximately expressed as:

$$V'(r) = I - A - C(r) \quad (12)$$

where I is the molecular ionization potential, A is the molecular electron affinity and $C(r)$ is the coulombic interaction between the positive and negative molecular ions.

So far the interactions between a ground-state chromophore and an excited-state chromophore are assumed to be isolated and in a vacuum. In general, the dispersion forces will become retarded at shorter distances than they do *in vacuo*. In a solution, the differences in interactions between phenyl–phenyl and phenyl–solvent must be considered. This effect is still present even if the chromophores are so close together that there is no room for solvent molecules between them. Because the excimer interaction energy gained by bringing together a pair of phenyl rings originally surrounded by heptane is lower than that for bringing together rings that are more stabilized by neighbouring PS segments, the excimer interaction potential energy V' should also be flattened. In this case, the resulting potential energy curve will become less steep, causing a band narrowing and a blue shift of the excimer band, as shown in *Figure 12*.

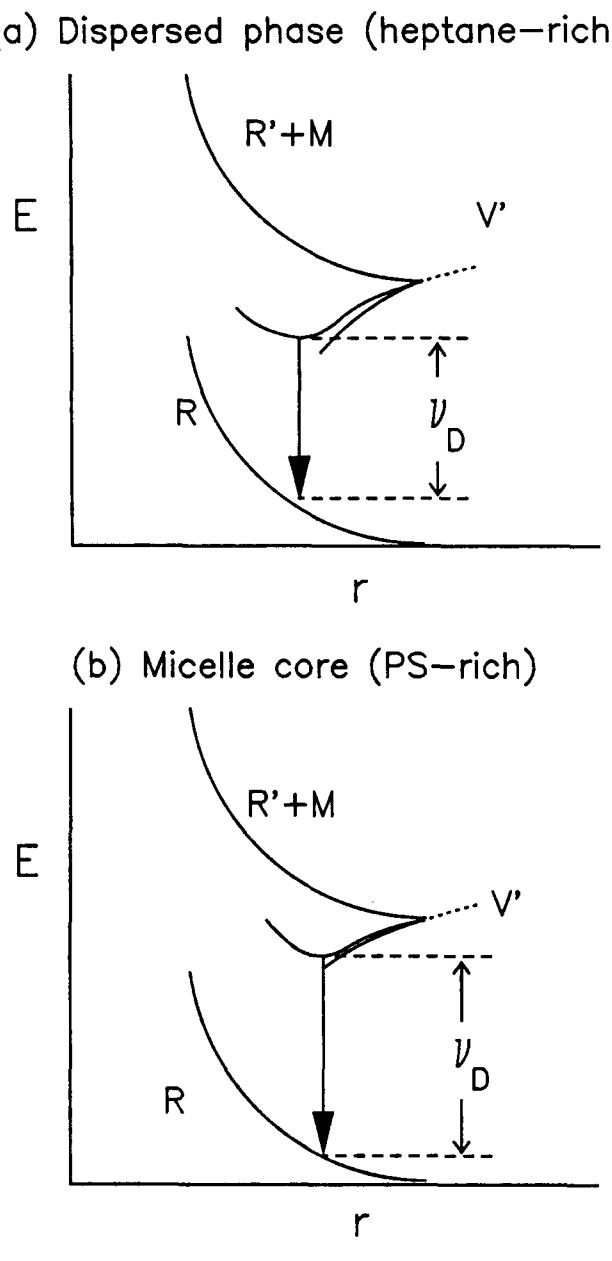

Figure 12 A schematic comparison of the potential energy diagrams for excimer formation of PS in (a) a heptane-rich environment and (b) a PS-rich environment

It is tempting to provide a more quantitative account for the bandwidth and band position changes in terms of differences in dielectric constant, and therefore repulsive interactions, coulombic interactions and ionization potential and electron affinity. However, the effective dielectric constant may be directional and not uniform on a molecular scale, and the changes in I and A are not easily measured. Therefore, we will confine ourselves to this qualitative explanation for the present study.

Transient fluorescence behaviour

Because of the high density of chromophores and therefore the expected facile extent of energy migration, we have adopted a judicious approach in the interpretation of the transient fluorescence data. We have chosen to comment qualitatively on the appearance of the monomer and excimer decay profiles, and have based our analysis on the changes in mean decay times. From the monomer fluorescence decay measurements, it is obvious that the PS segment density increases with concentration for $c=0.07$–1%. Furthermore, the absence of a rise time in the excimer decay profile at 1–2% provides excellent support for the existence of preformed excimer sites, in corroboration of the assumption that $\phi \sim 1$ for $c > c_I$. In comparison with the excimer fluorescence decay profiles for $c<3\%$, the excimer decay profile at 3% is less short-lived, indicating that excimer formation from the dispersed phase, where the PS segment density is still very low, begins to contribute to the overall I_D/I_M.

Micellar core and corona radii

Evidence of morphological changes as a function of concentration can be obtained from changes in I_D/I_M, $\Delta\nu_{D,1/2}$ and ν_D with concentration. As shown in *Figures 2, 3* and *4*, there are several distinct regions in which changes in these excimer fluorescence observables may shed light on the concentration dependence of the core morphology and the corona size.

At a concentration presumably close to the c.m.c. (below 0.01% for heptane solutions, for example) the rise in I_D/I_M with increasing concentration is accompanied by a blue shift of the excimer band as well as considerable band narrowing, indicative of a decrease in solvation of the PS core. As the concentration increases, the solvent molecules are increasingly driven out of the core, resulting in a shrinkage of the core, and hence a smaller hydrodynamic radius. Such changes in I_D/I_M, $\Delta\nu_{D,1/2}$ and ν_D from 0.001 to 0.01% are in agreement with the p.c.s. results obtained in paper 1[1], that the hydrodynamic radius is significantly reduced from $R=59$ nm at 0.003% to $R=46$ nm from 0.01 up to 0.07%.

Normally, a rise in I_D/I_M implies that the local PS segment density is increasing. Within the present context this would mean that fewer solvent molecules are residing within the micelle core. It is interesting to note that the increase in I_D/I_M is not accompanied by a decrease in hydrodynamic radius for $c=0.01$–0.07%. From *Table 3*, the volume fractions of PS in the core are estimated to be $\phi=0.50$ at 0.01% and $\phi=0.77$ at 0.07%. For a micellar core radius of $R_{core}=10$–15 nm[17,18], it would imply a reduction of only 1–3 nm in R_{core}.

The increase in I_D/I_M from 0.1 to 0.5% can be easily explained in terms of further enhancement in energy migration as the core becomes denser. However, such an observation can be obscured by the self-absorption effect. An examination of the excitation spectra indicates that self-absorption begins to play a significant role above 0.1%. Although we have attempted to correct for self-absorption by comparing and ratioing spectra measured with front-face and right-angle geometry, the concentration of micelles could become high enough that this effect is not eliminated entirely even with front-face illumination[21]. As shown in *Table 3*, the increase in excimer emission for the core from $I_D/I_M=13.5$ at 0.1% to $I_D/I_M=15.2$ at 0.5% does not give rise to any change in R_{core}. Hence, we believe the reduction of the apparent hydrodynamic radius from $R=44.9$ nm at 0.1% to $R=41.4$ nm at 0.5% (see table 1 in paper 1[1]) should be due to collective diffusion of micelles.

The decrease in I_D/I_M at 0.5% for heptane solutions ($\sim$0.25% for dodecane solutions) cannot be caused by self-absorption. On the contrary, changing the free chain–micelle equilibrium in favour of the free chains could easily explain such an increase in I_D/I_M since the

local PS segment density in a free chain should be considerably lower than that in the micelle core. Since I_D/I_M depends on the local concentration and mobility of phenyl rings, a change in free chain population could affect the extent and stability of the resulting excimer species. Rather intriguing is the fact that the presence of freely dispersed chains does not lead to an increase in excimer bandwidth, as in the concentration region of 0.001–0.007%. Since I_D/I_M is reduced following the presence of free chains in the dispersed phase, it is obvious that the excimer emission observed is due primarily to the facile excimer formation in the micellar core; and excimer emission from the free chains is relatively unimportant. This is also confirmed by the transient fluorescence results, where faster decay times, presumably due to the high PS segment density in the core, were observed for excimer emission with increasing concentration up to 2%.

At concentrations sufficiently higher than c_1, such as 1 or 2%, the solvent molecules are presumably excluded from the core, and the PS chains may be perturbed by the constraints of uniform density and chain placement at the corona–core interface. It appears that such an effect has brought about some preformed excimer sites, considering that the phenyl rings are packed very closely together, especially at 1–2%. Indeed, the absence of a rise time in transient excimer decay curves for 1 and 2% solutions provides support for this postulate. Windle *et al.*[22] have previously proposed from their X-ray study of PS films that stacking of phenyl rings is a distinct possibility in some cases. It is natural that an association of phenyl rings should provide an increase in the probability of preformed excimer sites.

The increase in I_D/I_M above 2% can be interpreted as a direct result of an increase in the volume fraction of PS in the dispersed or matrix phase, as the contribution of this increase in the local PS segment density in the free chains for $c>2\%$ has been illustrated in the calculation of X_R above. From the transient fluorescence at 3%, the excimer decay profile is quite different in appearance from those at 1 and 2%. In addition, the mean decay time increases from $\langle\tau\rangle=20.3$ ns at 1 and 2% to $\langle\tau\rangle=24.0$ ns at 3%, indicating that the kinetics of excimer formation is slower at 3% than at 1 and 2%. A possible explanation for this observation is that energy migration in the dispersed phase is less efficient than that in the core, resulting in a reduction of $\langle\tau\rangle$.

Temperature dependence of I_D/I_M, $\Delta\nu_{D,1/2}$ and ν_D

The intrinsic fluorescence behaviour, as exhibited by the temperature dependence of I_D/I_M, $\Delta\nu_{D,1/2}$ and ν_D, can be used to provide further information on the microstructure of the micellar core. The increase of excimer bandwidth with temperature is rather gradual, indicating that the solvent content within the core does not change rapidly. The fact that no transitions observed in the I_D/I_M plot are seen here suggests that I_D/I_M is more sensitive to changes in the local environment that pertain to excimer formation, such as ring–ring separation distances and chain mobility. Above the critical micelle temperature, however, the micelles no longer exist and the phenyl rings are now more strongly influenced by the solvent molecules. Such an abrupt change in local environment allows the excimer bandwidth to be used to measure the c.m.t. with more precision than I_D/I_M or excimer band position. Similarly, the excimer band position also changes with temperature. The red shift of excimer bands with increasing temperature is expected since a more stable excimer species can be expected with the increase in free volume for bond rotation.

The increase in I_D/I_M at 305–310 K is rather reproducible, but it does not correspond to any changes in morphology as probed by light scattering, neutron scattering, or nuclear magnetic resonance. Such an increase in I_D/I_M cannot be caused by an enhancement in excimer formation in unimers because a similar effect is observed in the 0.1% dodecane solution in which the presence of free chains is insignificant. An alternative explanation is that the increase in temperature lowers the segregation power of PS and PEP blocks, thereby increasing the mixing of PS and PEP blocks at the interface. Also, the thermal energy could induce a somewhat higher concentration of solvent molecules at the interface, which has now become more diffuse.

The observation of a jump in I_D/I_M at 330–350 K may herald the onset of the solvation of the micelle core. According to n.m.r. measurements on a similar PSPEP in octane[23], a sharp linewidth transition of the rigid component at 323 K was attributed to the plasticization of the PS matrix by solvent molecules within the core. On the other hand, small-angle X-ray scattering and rheology measurements[24] suggest that a loss of long-range order of micelles, i.e. a transition from macrolattice to a randomly spaced superstructure, may occur in this region. Watanabe *et al.*[24] pointed out that the solvation of the micelle core and the loss of long-range order are usually interrelated and should therefore occur simultaneously. At the present time, we will attribute such a rise in I_D/I_M to the solvation of the core.

While the c.m.t. is higher for a more concentrated solution, regardless of the existence of free chains in the solutions, the existence of free chains may complicate the analysis. The fact that I_D/I_M in the 0.1% PSPEP solution in dodecane is higher than that in the 1 or 2% solution at any particular temperature indicates that the free chain–micelle equilibrium dictates the extent of solvation within the micellar core. Such an effect manifests itself strongly at the critical micelle temperature. It is unclear whether the free chain–micelle equilibrium is altered such that fewer free chains are present at high temperatures. The dissociation of micelles at the c.m.t. is somewhat gradual, in agreement with the suggestion by Watanabe[24].

SUMMARY

The technique of excimer fluorescence can be used to measure the critical micelle temperature of PSPEP block copolymer micelles. Using a three-dimensional energy migration lattice model, the volume fraction of PS segments in the micelle core can be estimated. Photostationary and transient fluorescence results confirm the presence of free chains in the dispersed phase at sufficiently high concentrations. The amount of freely dispersed chains appears to be higher at $c=2\%$ than at $c=0.7\%$.

ACKNOWLEDGEMENTS

We thank David Ylitalo for many helpful discussions and for preparing some of the sample solutions in dodecane. This work was supported by Shell Development Co.

REFERENCES

1 Yeung, A. S. and Frank, C. W. *Polymer* 1990, **31**, 2089
2 Gelles, R. and Frank, C. W. *Macromolecules* 1983, **16**, 1448
3 Gelles, R. and Frank, C. W. *Macromolecules* 1982, **15**, 741
4 Liano, P. and Zana, R. *J. Phys. Chem.* 1980, **84**, 3339
5 Liano, P., Viriot, M. and Zana, R. *J. Phys. Chem.* 1984, **88**, 1098
6 Malliaris, A., Le Moigne, J., Sturm, J. and Zana, R. *J. Phys. Chem.* 1985, **89**, 2709
7 Turro, N. J. and Kuo, P. *J. Phys. Chem.* 1987, **91**, 3321
8 Fitzgibbon, P. D. and Frank, C. W. *Macromolecules* 1981, **14**, 1650
9 Miller, J. N. (Ed.) 'Standards in Fluorescence Spectroscopy', Chapman and Hall, New York, 1981
10 Hemker, D. J., Frank, C. W. and Thomas, J. W. *Polymer* 1988, **29**, 437
11 Tuzar, Z. and Kratochvil, P. *Adv. Colloid Interface Sci.* 1976, **6**, 201
12 Phillips, D., Roberts, A. J., Rumbles, G. and Soutar, I. *Macromolecules* 1983, **16**, 1597
13 Fredrickson, G. H. and Frank, C. W. *Macromolecules* 1984, **17**, 54
14 Price, C., Kendall, K. D., Stubberfield, R. B. and Wright, B. *Polym. Commun.* 1983, **24**, 326
15 Price, C., Chan, E. K. M., Mobbs, R. H. and Stubberfield, R. B. *Eur. Polym. J.* 1985, **21**, 355
16 Birks, J. B. 'Photophysics of Aromatic Molecules', Wiley, New York, 1970
17 Higgins, J. S., Blake, S., Tomlins, P. E., Ross-Murphy, S. B., Staples, E., Penfold, J. and Dawkins, J. V. *Polymer* 1989, **29**, 1968
18 Higgins, J. S., Dawkins, J. V., Maghami, G. G. and Shakir, S. A. *Polymer* 1986, **27**, 931
19 Berlman, I. B. 'Energy Transfer Parameters of Aromatic Compounds', Academic Press, New York, 1972
20 Birks, J. B. and Christophorus, L. G. *Proc. R. Soc.* (*A*) 1964, **277**, 571
21 Tsai, F. J. and Torkelson, J. M. *Polymer* 1988, **29**, 1005
22 Mitchell, G. R. and Windle, A. H. *Polymer* 1984, **25**, 906
23 Candau, F., Heatley, F., Price, C. and Stubberfield, R. B. *Eur. Polym. J.* 1984, **20**, 685
24 Watanabe, H. and Kotaka, T. *Polym. Eng. Rev.* 1984, **4**, 1